

**HYBRID SOLID-PLATE QUADRILATERALS.  
AN ASSESSMENT AND NEW DEVELOPMENTS**

**G.M. Kulikov, S.V. Plotnikova**

*Department of Applied Mathematics and Mechanics, TSTU*

**Key words and phrases:** assumed natural strain method; four-node solid-plate element; hybrid finite element models.

**Abstract:** On the basis of the first-order solid-plate theory, proposed in earlier authors' papers, the hybrid stress, strain and stress-strain quadrilateral ANS four-node plate elements are developed. All hybrid solid-plate elements are based on the unified technique that gives an opportunity to assess their advantages and disadvantages. For instance, a hybrid stress-strain quadrilateral ANS element permits the analytical integration, which leads to a very simple structure of its stiffness matrix. At the same time the hybrid stress ANS quadrilateral exhibits a superior performance in all plate problems considered but requires a numerical large size matrix inversion.

---

## 1. Introduction

A displacement-based four-node solid-plate element formulation based on the assumed natural strain (ANS) method has been proposed in [1]. To improve the computational efficiency of the displacement-based ANS low-order plate/shell elements, a hybrid method can be applied. This method is based on the robust finite element formulation pioneered by Pian [2]. In such a formulation the displacements on the element boundary are assumed to provide displacement compatibility between elements, whereas internal stresses are assumed so as to satisfy the differential equilibrium equations. The Pian's work was originally based upon the principle of the stationary complementary energy. Later, an alternative assumed stress method was proposed by applying the Hellinger-Reissner variational principle that simplifies the evaluation of the element stiffness matrix [3].

However, herein we do not use this terminology referring to Gallagher's proposal (see paper [4]), where it is said that "the hybrid method in structural mechanics is defined at the one which is formulated by multivariable variational functional, yet the resulting matrix equations consist of only the nodal values of displacements as unknown". Independently, the hybrid strain [5] and hybrid stress-strain [6] shell elements were developed. The former is based on the modified Hellinger-Reissner functional in which displacements and strains are utilized as fundamental shell unknowns, whereas the latter departs from the Hu-Washizu functional depending on displacements, stresses and strains.

In the present paper, all three hybrid ANS four-node plate elements are studied by using a unified technique. This allows one to assess their advantages and disadvantages and to compare them with a displacement-based ANS plate element [1]. In this context, we notice that a hybrid stress-strain ANS plate element permits the analytical integration of some matrices that yields the simple analytical matrix inversion [1]. At the same time the hybrid stress and hybrid strain ANS plate elements exhibit an excellent performance in all benchmark problems considered but require expensive numerical matrix inversions.

## 2. Hybrid stress-strain ANS solid-plate element

To develop the hybrid stress-strain finite element formulation, we have to invoke the Hu-Washizu variational principal in which displacements, strains and stresses are utilized as independent variables. Inserting distributions of displacements, displacement-dependent and displacement-independent strains through the thickness of the plate [1] into the 3D Hu-Washizu functional, one finds

$$\iint_{\Omega_{el}} [\delta \mathbf{E}^T (\mathbf{D}\mathbf{E} - \mathbf{H}) + \delta \mathbf{H}^T (\boldsymbol{\varepsilon} - \mathbf{E}) + \delta \boldsymbol{\varepsilon}^T \mathbf{H} - \delta \mathbf{u}^T \boldsymbol{\mathcal{P}}] dx^1 dx^2 - \delta W_{el}^{ext} = 0, \quad (1)$$

$$\mathbf{u} = [u_1^- \ u_1^+ \ u_2^- \ u_2^+ \ u_3^- \ u_3^+]^T, \quad \boldsymbol{\mathcal{P}} = [-p_1^- \ p_1^+ \ -p_2^- \ p_2^+ \ -p_3^- \ p_3^+]^T, \quad (2)$$

$$\boldsymbol{\varepsilon} = [\varepsilon_{11}^- \ \varepsilon_{11}^+ \ \varepsilon_{22}^- \ \varepsilon_{22}^+ \ 2\varepsilon_{12}^- \ 2\varepsilon_{12}^+ \ 2\varepsilon_{13}^- \ 2\varepsilon_{13}^+ \ 2\varepsilon_{23}^- \ 2\varepsilon_{23}^+ \ \bar{\varepsilon}_{33}]^T,$$

$$\mathbf{E} = [E_{11}^- \ E_{11}^+ \ E_{22}^- \ E_{22}^+ \ 2E_{12}^- \ 2E_{12}^+ \ 2E_{13}^- \ 2E_{13}^+ \ 2E_{23}^- \ 2E_{23}^+ \ E_{33}]^T,$$

$$\mathbf{H} = [H_{11}^- \ H_{11}^+ \ H_{22}^- \ H_{22}^+ \ H_{12}^- \ H_{12}^+ \ H_{13}^- \ H_{13}^+ \ H_{23}^- \ H_{23}^+ \ H_{33}]^T,$$

where  $u_i^-$  and  $u_i^+$  are the components of displacement vectors  $\mathbf{u}^-$  and  $\mathbf{u}^+$  of the bottom and top planes;  $p_i^-$  and  $p_i^+$  are the components of surface traction vectors  $\mathbf{p}^-$  and  $\mathbf{p}^+$  applied to the bottom and top planes;  $W_{el}^{ext}$  is the work done by external loads acting on the boundary surface  $\Sigma_{el}$ ;  $\varepsilon_{\alpha\beta}^\pm$ ,  $\varepsilon_{\alpha 3}^\pm$  and  $\bar{\varepsilon}_{33}$  are the in-plane, transverse shear and transverse normal components of the displacement-dependent strain tensors;  $E_{\alpha\beta}^\pm$ ,  $E_{\alpha 3}^\pm$  and  $E_{33}$  are the in-plane, transverse shear and transverse normal components of the displacement-independent strain tensors;  $H_{\alpha\beta}^\pm$ ,  $H_{\alpha 3}^\pm$  and  $H_{33}$  are the components of the stress resultant tensors;  $\mathbf{D}$  is the constitutive stiffness matrix of order  $11 \times 11$  [7] whose components are found in accordance with the simplest remedy of S.W. Lee et al. [8] to prevent thickness locking; indices  $i, j$  take the values 1, 2 and 3, whereas indices  $\alpha, \beta$  take the values 1 and 2. We refer to (1) as a Hu-Washizu variational equation. A short discussion on that is presented in Appendix A.

For the isoparametric quadrilateral four-node solid-plate element (Fig. 1) the position vector in the initial configuration and the displacement vector are approximated according to the standard  $C^0$  interpolation

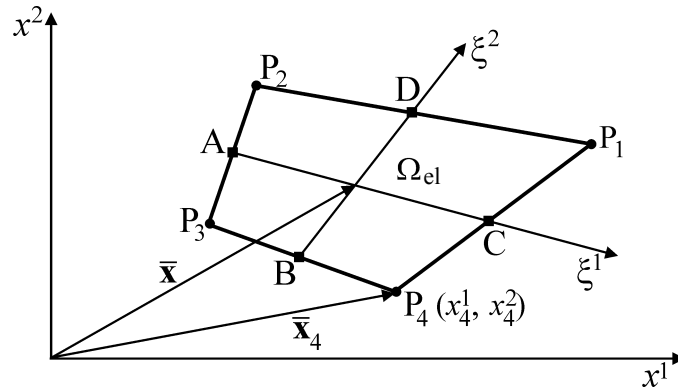


Fig. 1. Quadrilateral plate element

$$\bar{\mathbf{x}} = \sum_r N_r \bar{\mathbf{x}}_r, \quad \bar{\mathbf{x}} = [x^1 \ x^2 \ 0]^T, \quad \bar{\mathbf{x}}_r = [x_r^1 \ x_r^2 \ 0]^T, \quad (3)$$

$$\mathbf{u} = \sum_r N_r \mathbf{u}_r, \quad \mathbf{u}_r = [u_{1r}^- \ u_{1r}^+ \ u_{2r}^- \ u_{2r}^+ \ u_{3r}^- \ u_{3r}^+]^T, \quad (4)$$

where  $\mathbf{u}_r$  are the displacement vectors of the element nodes;  $N_r(\xi^1, \xi^2)$  are the bilinear shape functions of the element;  $\xi^\alpha$  are the natural coordinates; the index  $r$  runs from 1 to 4 and denotes a number of nodes.

In order to avoid shear locking, we employ the ANS method using its non-conventional treatment [1] that leads in conjunction with displacement interpolation (4) to

$$\boldsymbol{\varepsilon} = \mathbf{B}\mathbf{U}, \quad \mathbf{U} = [\mathbf{u}_1^T \ \mathbf{u}_2^T \ \mathbf{u}_3^T \ \mathbf{u}_4^T]^T, \quad (5)$$

where  $\mathbf{U}$  is the displacement vector of the solid-plate element;  $\mathbf{B}$  is the strain-displacement transformation matrix of order  $11 \times 24$ .

In order to fulfill a patch test, the assumed stress resultants and displacement-independent strains are interpolated throughout the element following ideas [3, 9]

$$\mathbf{H} = \mathbf{P}_H \boldsymbol{\psi}, \quad \boldsymbol{\psi} = [\psi_1 \ \psi_2 \ \dots \ \psi_{22}]^T, \quad (6)$$

$$\mathbf{E} = \mathbf{P}_E \boldsymbol{\varphi}, \quad \boldsymbol{\varphi} = [\varphi_1 \ \varphi_2 \ \dots \ \varphi_{22}]^T, \quad (7)$$

where  $\mathbf{P}_H$  and  $\mathbf{P}_E$  are the matrices of order  $11 \times 22$  depending on natural coordinates  $\xi^\alpha$  [1].

Using interpolations (3) – (7) in the variational equation (1), the following equilibrium equations are obtained:

$$\mathbf{Q}^T \boldsymbol{\psi} = \mathbf{G}_E \boldsymbol{\varphi}, \quad \mathbf{Q} \boldsymbol{\varphi} = \mathbf{R}_H \mathbf{U}, \quad \mathbf{R}_H^T \boldsymbol{\psi} = \mathbf{F}. \quad (8)$$

Here,  $\mathbf{F}$  is the force vector and

$$\mathbf{G}_E = \int_{-1}^1 \int_{-1}^1 \mathbf{P}_E^T \mathbf{D} \mathbf{P}_E \Lambda d\xi^1 d\xi^2, \quad \mathbf{R}_H = \int_{-1}^1 \int_{-1}^1 \mathbf{P}_H^T \mathbf{B} \Lambda d\xi^1 d\xi^2, \quad (9)$$

$$\mathbf{Q} = \int_{-1}^1 \int_{-1}^1 \mathbf{P}_H^T \mathbf{P}_E \Lambda d\xi^1 d\xi^2,$$

where  $\Lambda$  is the determinant of the Jacobian matrix defined as

$$\Lambda = c_0 + c_1 \xi^1 + c_2 \xi^2, \quad (10)$$

$$c_0 = \frac{1}{8} [(x_1^1 - x_3^1)(x_2^2 - x_4^2) - (x_2^1 - x_4^1)(x_1^2 - x_3^2)],$$

$$c_1 = \frac{1}{8} [(x_1^1 - x_2^1)(x_3^2 - x_4^2) - (x_3^1 - x_4^1)(x_1^2 - x_2^2)],$$

$$c_2 = \frac{1}{8} [(x_1^1 - x_4^1)(x_2^2 - x_3^2) - (x_2^1 - x_3^1)(x_1^2 - x_4^2)].$$

Eliminating assumed stress and strain parameter vectors  $\boldsymbol{\psi}$  and  $\boldsymbol{\phi}$  from elemental equations (8), we arrive at the governing equations

$$\mathbf{K}_{EH}\mathbf{U} = \mathbf{F}, \quad (11)$$

where  $\mathbf{K}_{EH}$  denotes the element stiffness matrix given by

$$\mathbf{K}_{EH} = \mathbf{R}_H^T \mathbf{Q}^{-1} \mathbf{G}_E \mathbf{Q}^{-1} \mathbf{R}_H. \quad (12)$$

Because of a simple structure of the matrix  $\mathbf{Q}$ , its inversion can be readily fulfilled in a closed form [1]. Thus, no expensive numerical matrix inversion is needed if one uses the hybrid stress-strain method.

### 3. Hybrid stress ANS solid-plate element

The hybrid stress finite element formulation is based on the Hellinger-Reissner variational principle, which can be expressed in our notations (2) as

$$\iint_{\Omega_{el}} [\delta \mathbf{H}^T (\boldsymbol{\varepsilon} - \mathbf{D}^{-1} \mathbf{H}) + \delta \boldsymbol{\varepsilon}^T \mathbf{H} - \delta \mathbf{u}^T \mathcal{P}] dx^1 dx^2 - \delta W_{el}^{ext} = 0. \quad (13)$$

We refer to (13) as a Hellinger-Reissner variational equation (see Appendix A).

The use of interpolations (3) – (6) in the mixed variational equation (13) leads to equilibrium equations

$$\mathbf{R}_H \mathbf{U} = \mathbf{G}_H \boldsymbol{\psi}, \quad \mathbf{R}_H^T \boldsymbol{\psi} = \mathbf{F}, \quad (14)$$

where

$$\mathbf{G}_H = \int_{-1}^1 \int_{-1}^1 \mathbf{P}_H^T \mathbf{D}^{-1} \mathbf{P}_H \Lambda d\xi^1 d\xi^2. \quad (15)$$

Due to the fact that stress resultants (6) are interpolated discontinuously across element boundaries, the assumed stress parameter vector  $\boldsymbol{\psi}$  can be eliminated at the element level and we arrive at the pure displacement-based problem

$$\mathbf{K}_H \mathbf{U} = \mathbf{F}, \quad (16)$$

where  $\mathbf{K}_H$  denotes the element stiffness matrix given by

$$\mathbf{K}_H = \mathbf{R}_H^T \mathbf{G}_H^{-1} \mathbf{R}_H. \quad (17)$$

It is seen that the hybrid stress plate element formulation requires a numerical inversion of the matrix of order  $22 \times 22$ .

### 4. Hybrid strain ANS solid-plate element

The hybrid strain finite element formulation is based on the modified Hellinger-Reissner functional in which displacements and strains are utilized as fundamental shell unknowns. Therefore, taking into account the distribution of strains through the

thickness of the shell [1] and using constitutive equations into the aforementioned 3D mixed functional, we represent the 2D modified Hellinger-Reissner variational equation in the following form:

$$\iint_{\Omega_{el}} [\delta \mathbf{E}^T \mathbf{D}(\boldsymbol{\varepsilon} - \mathbf{E}) + \delta \boldsymbol{\varepsilon}^T \mathbf{D} \mathbf{E} - \delta \mathbf{u}^T \mathcal{P}] dx^1 dx^2 - \delta W_{el}^{ext} = 0. \quad (18)$$

Substituting interpolations (3) – (5) and (7) in the mixed variational equation (18) and recalling notations (9), we derive the elemental equilibrium equations

$$\mathbf{R}_E \mathbf{U} = \mathbf{G}_E \boldsymbol{\varphi}, \quad \mathbf{R}_E^T \boldsymbol{\varphi} = \mathbf{F}, \quad (19)$$

where

$$\mathbf{R}_E = \int_{-1}^1 \int_{-1}^1 \mathbf{P}_E^T \mathbf{D} \mathbf{B} \Lambda d\xi^1 d\xi^2. \quad (20)$$

Since the assumed strain interpolations (7) are discontinuous at the element boundaries, a static condensation on the element level yields the element stiffness matrix

$$\mathbf{K}_E = \mathbf{R}_E^T \mathbf{G}_E^{-1} \mathbf{R}_E. \quad (21)$$

Thus, again a pure displacement-based problem

$$\mathbf{K}_E \mathbf{U} = \mathbf{F} \quad (22)$$

has to be solved.

One can see that the hybrid strain plate element formulation also leads to the numerical inversion of the matrix of order  $22 \times 22$ .

**Remark.** Using a link between transverse components of the displacement-dependent strain tensor and following a technique [10], one can derive *four* coupling conditions for the transverse components of the displacement-independent strain tensor. These conditions imply that only 18 assumed strain parameters are *independent* of 22 ones introduced by approximation (7). As a result, the elemental stiffness matrices of all hybrid methods developed, namely,  $\mathbf{K}_{EH}$ ,  $\mathbf{K}_H$  and  $\mathbf{K}_E$  have six, and only six, zero eigenvalues as required for satisfaction of the general rigid-body motion representation, since 24 displacement degrees of freedom are introduced. Note that integrals are calculated by applying a Gauss numerical integration scheme with  $2 \times 2$  integration points.

## 5. Numerical examples

The performance of the proposed quadrilateral four-node solid-plate elements is evaluated with several problems extracted from the literature. A listing of these elements and the abbreviations used to identify them are contained in Table 1.

### 5.1. Cook's membrane problem

A trapezoidal plate is clamped on one side while the opposite side is subjected to a distributed in-plane load as shown in Fig. 2. This test is an excellent ability to verify a proper representation of the membrane dominated stress state with skewed meshes.

Table 2 lists the normalized in-plane tip displacement of the midplane  $(u_2^M)^{\text{Norm}}$ . For this purpose a converged finite element solution of 23.91 [9] has been used. As turned out, the SPQ4 $\epsilon$  element finished with the lowest rank among all mixed solid-plate elements developed.

## 5.2. Simply supported square plate under central load

This problem is invoked to test the effect of mesh distortion on the performance of proposed solid-plate elements. A quarter of the simply supported square plate subjected to a concentrated load is modeled by a coarse  $2 \times 2$  mesh. The geometrical and

Table 1

**Listing of quadrilateral four-node solid-plate elements**

| Name                  | Description  |
|-----------------------|--|
| SPQ4                  | Solid-plate quadrilateral based on the displacement-based ANS formulation [1]              |
| SPQ4 $\sigma\epsilon$ | Solid-plate quadrilateral based on the consistent hybrid stress-strain ANS formulation [1] |
| SPQ4 $\sigma$         | Solid-plate quadrilateral based on the hybrid stress ANS formulation (section 3)           |
| SPQ4 $\epsilon$       | Solid-plate quadrilateral based on the hybrid strain ANS formulation (section 4)           |

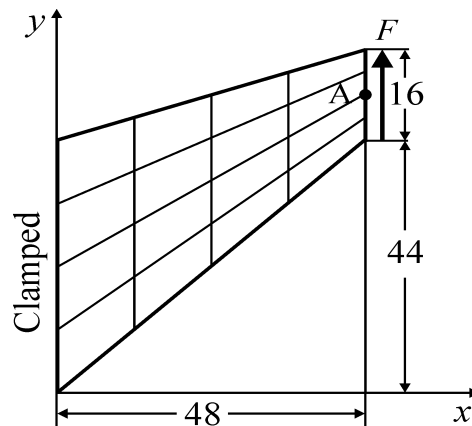


**Fig. 2. Cook's membrane problem:**  
 $h = 1; E = 1; \nu = 0.33; F = 1$

Table 2

**Normalized in-plane tip displacement of trapezoidal plate**

| Mesh           | SPQ4   | SPQ4 $\sigma\epsilon$ | SPQ4 $\sigma$ | SPQ4 $\epsilon$ | Simo [9] |
|----------------|--------|-----------------------|---------------|-----------------|----------|
| $2 \times 2$   | 0.4954 | 0.7332                | 0.8835        | 0.5555          | 0.883    |
| $4 \times 4$   | 0.7654 | 0.9126                | 0.9627        | 0.8120          | 0.963    |
| $8 \times 8$   | 0.9234 | 0.9760                | 0.9906        | 0.9421          | 0.991    |
| $16 \times 16$ | 0.9798 | 0.9948                | 0.9987        | 0.9853          | 0.999    |

mechanical data of the problem are displayed in Fig. 3. The mesh is distorted by moving the inner node along the diagonal of the upper right square. In such situation a Jacobian may be written according to (10) as

$$\Lambda = \frac{1}{4} \left( 1 - \Delta + \frac{1}{2} \Delta \xi^1 + \frac{1}{2} \Delta \xi^2 \right). \quad (23)$$

Taking into account (23), one can represent Jacobian values at the crucial Gauss point as a function of the parameter  $\Delta$ :

$$\Lambda \left( -\frac{1}{\sqrt{3}}, -\frac{1}{\sqrt{3}} \right) = \begin{cases} \text{positive for } \Delta = 0.6, \\ \text{zero for } \Delta = \sqrt{3}/(\sqrt{3}+1) = 0.6340, \\ \text{negative for } \Delta = 0.7. \end{cases}$$

Table 3 displays the transverse central displacement of the midplane  $u_3^M$  normalized with respect to the analytical solution [11] of  $0.01160 Fa^2/D$  based on the Kirchhoff plate theory. It is seen that all hybrid solid-plate elements perform excellently even in the case of a negative Jacobian. As mentioned in [9], it is an unacceptable situation for practical implementations of course.

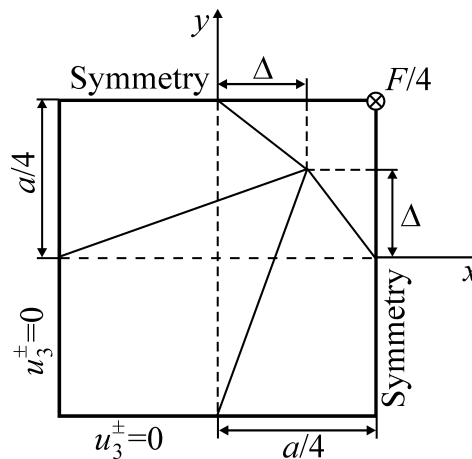


**Fig. 3. Simply supported square plate under central load:**  
 $a = 4; h = 0.004; E = 1.092 \times 10^6; \nu = 0.3; F = 10^{-5}$

Table 3

**Normalized transverse center point displacement of square plate**

| $\Delta$ | SPQ4   | SPQ4 $\sigma\epsilon$ | SPQ4 $\sigma$ | SPQ4 $\epsilon$ | Simo [9] |
|----------|--------|-----------------------|---------------|-----------------|----------|
| 0.0      | 0.9922 | 1.0042                | 1.0074        | 1.0042          | 1.002    |
| 0.1      | 0.9871 | 0.9990                | 1.0026        | 0.9986          | 0.998    |
| 0.2      | 0.9768 | 0.9871                | 0.9917        | 0.9886          | 0.988    |
| 0.3      | 0.9609 | 0.9676                | 0.9739        | 0.9739          | 0.972    |
| 0.4      | 0.9378 | 0.9395                | 0.9483        | 0.9536          | 0.949    |
| 0.5      | 0.9048 | 0.9007                | 0.9139        | 0.9257          | 0.918    |
| 0.6      | 0.8511 | 0.8480                | 0.8697        | 0.8865          | 0.879    |
| 0.7      | fail   | 0.7802                | 0.8126        | 0.8256          | –        |

### 5.3. Simply supported rhombic plate under uniform pressure

A simply supported rhombic plate with a skew angle  $30^\circ$  is subjected to uniformly distributed transverse loading. This problem is particularly challenging due to the fact that moments at the obtuse corners are singular. The plate is discretized with regular meshes as shown in Fig. 4.

The normalized transverse central displacement of the midplane  $(u_3^M)^{\text{Norm}}$  is listed in Table 4. The analytical Morley's solution [13] of 0.04455 has been used to normalize the derived results. All proposed ANS solid-plate elements exhibit a superior performance except for the hybrid stress-strain SPQ4 $\sigma\epsilon$  element, which lags behind in the case of coarse mesh configurations.

### 5.4. Circular plate under central load

Consider a thin circular plate subjected to a concentrated load at the center point. The mechanical and geometrical characteristics of the plate are given in Fig. 5. The standard meshes are used to model due to symmetry only one quarter of the plate.

Table 5 lists the transverse central midplane displacements  $u_3^M$  of the simply supported and clamped plates normalized with respect to the analytical solutions [11]

$$u_3^{\text{SS}} = \frac{(3+\nu)FR^2}{16\pi(1+\nu)D} \quad \text{and} \quad u_3^{\text{CL}} = \frac{FR^2}{16\pi D}$$

based on the Kirchhoff plate theory. As can be seen, the developed SPQ4 $\sigma$  and SPQ4 $\epsilon$  elements are the best performers again although the other ANS solid-plate elements [1] work well.

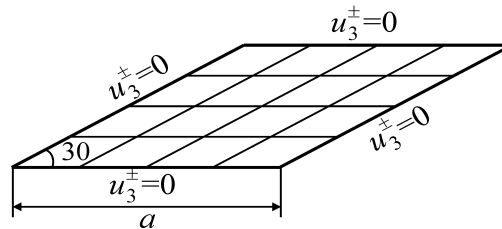


Fig. 4. Simply supported rhombic plate under uniform pressure:  
 $a = 100; h = 1; E = 10^7; \nu = 0.3; p = 1$

Table 4

Normalized transverse center point displacement of rhombic plate

| Mesh           | SPQ4   | SPQ4 $\sigma\epsilon$ | SPQ4 $\sigma$ | SPQ4 $\epsilon$ | Simo [9] | MITC4 [12] |
|----------------|--------|-----------------------|---------------|-----------------|----------|------------|
| 4 $\times$ 4   | 0.8791 | 0.6269                | 0.9463        | 1.0176          | 0.961    | 0.879      |
| 8 $\times$ 8   | 0.8714 | 0.7724                | 0.9540        | 0.9840          | 0.957    | 0.871      |
| 16 $\times$ 16 | 0.9382 | 0.8895                | 0.9911        | 0.9678          | 0.985    | 0.933      |
| 32 $\times$ 32 | 0.9952 | 0.9681                | 1.0188        | 1.0054          | 1.009    | 0.985      |



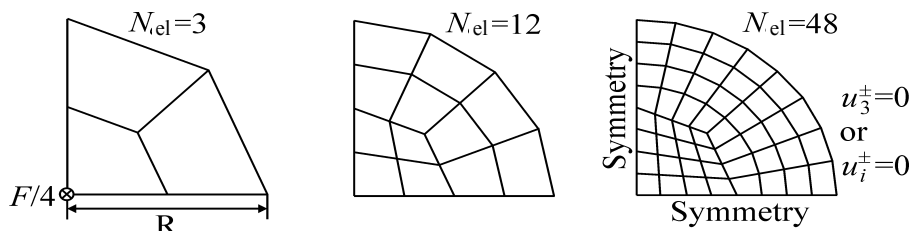


Fig. 5. Circular plate under central load:  
 $R = 1000$ ;  $h = 1$ ;  $E = 2 \times 10^6$ ;  $\nu = 0.3$ ;  $F = 1$

Table 5

Normalized transverse center point displacement of circular plate

| $N_{el}$ | Simply supported plate |                       |               |                 | Clamped plate |                       |               |                 |
|----------|------------------------|-----------------------|---------------|-----------------|---------------|-----------------------|---------------|-----------------|
|          | SPQ4                   | SPQ4 $\sigma\epsilon$ | SPQ4 $\sigma$ | SPQ4 $\epsilon$ | SPQ4          | SPQ4 $\sigma\epsilon$ | SPQ4 $\sigma$ | SPQ4 $\epsilon$ |
| 3        | 0.9831                 | 0.9892                | 0.9905        | 0.9894          | 0.7865        | 0.8022                | 0.8049        | 0.8022          |
| 12       | 0.9956                 | 0.9964                | 0.9982        | 0.9986          | 0.9484        | 0.9507                | 0.9551        | 0.9559          |
| 48       | 0.9984                 | 0.9988                | 0.9992        | 0.9992          | 0.9860        | 0.9869                | 0.9881        | 0.9881          |

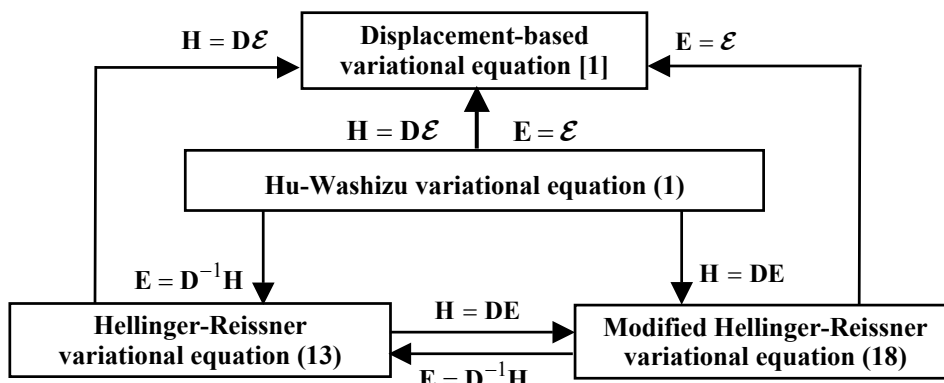


Fig. 6. Interconnection of used variational equations

## 6. Conclusions

On the basis of the first-order solid-plate theory [1, 14] accounting for thickness stretching the hybrid stress and hybrid strain ANS quadrilateral solid-plate elements have been developed. It is worth noting that stiffness matrices of the proposed hybrid solid-plate elements have six zero eigenvalues as required for satisfaction of the general rigid-body motion representation. The extension of the hybrid ANS quadrilateral solid-plate elements to the geometrically exact solid-shell quadrilaterals is currently under development and will be reported in the next papers.

## Appendix A

Finally, we describe an interconnection between displacement-based [1] and mixed variational equations employed in the present paper for development of the hybrid four-node solid-plate quadrilaterals. They are displayed in Fig. 6.

*The present research was supported by Russian Foundation for Basic Research (Grant No. 08-01-00373).*

## References

1. Kulikov, G.M. Assumed stress-strain quadrilateral plate elements based on analytical and numerical integration / G.M. Kulikov, S.V. Plotnikova // Вестн. Тамб. гос. техн. ун-та. – 2006. – Т. 12, № 1А. – С. 107–121.
2. Pian, T.H.H. Derivation of element stiffness matrices by assumed stress distributions / T.H.H. Pian // AIAA Journal. – 1964. – Vol. 2. – P. 1333–1336.
3. Pian, T.H.H. Rational approach for assumed stress finite elements / T.H.H. Pian, K. Sumihara // International Journal for Numerical Methods in Engineering. – 1984. – Vol. 20. – P. 1685–1695.
4. Pian, T.H.H. State-of-the-art development of hybrid/mixed finite element method / T.H.H. Pian // Finite Elements in Analysis and Design. – 1995. – Vol. 21. – P. 5–20.
5. Lee, S.W. Improvement of plate and shell finite elements by mixed formulations / S.W. Lee, T.H.H. Pian // AIAA Journal. – 1978. – Vol. 16. – P. 29–34.
6. Wempner, G. A simple and efficient approximation of shells via finite quadrilateral elements / G. Wempner, D. Talaslidis, C.M. Hwang // Trans. ASME. Journal of Applied Mechanics. – 1982. – Vol. 49. – P. 115–120.
7. Kulikov G.M. Geometrically exact assumed stress-strain multilayered solid-shell elements based on the 3D analytical integration / G.M. Kulikov, S.V. Plotnikova // Computers & Structures. – 2006. – Vol. 84. – P. 1275–1287.
8. Park, H.C. An efficient assumed strain element model with six dof per node for geometrically nonlinear shells / H.C. Park, C. Cho, S.W. Lee // International Journal for Numerical Methods in Engineering. – 1995. – Vol. 38. – P. 4101–4122.
9. Simo, J.C. On a stress resultant geometrically exact shell model. Part II: The linear theory; computational aspects / J.C. Simo, D.D. Fox, M.C. Rifai // Computer Methods in Applied Mechanics and Engineering. – 1989. – Vol. 73. – P. 53–92.
10. Kulikov, G.M. Equivalent single-layer and layer-wise shell theories and rigid-body motions. Part II : Computational aspects / G.M. Kulikov, S.V. Plotnikova // Mechanics of Advanced Materials and Structures. – 2005. – Vol. 12. – P. 331–340.
11. Timoshenko, S.P. Theory of Plates and Shells, 2nd ed. / S.P. Timoshenko, S. Woinowsky-Krieger. – New York : McGraw-Hill, 1970.
12. Bathe, K.J. A formulation of general shell elements – the use of mixed interpolation of tensorial components / K.J. Bathe, E.N. Dvorkin // International Journal for Numerical Methods in Engineering. – 1986. – Vol. 22. – P. 697–722.
13. Morley, L.S.D. Skew Plates and Structures / L.S.D. Morley. – New York : MacMillan, 1963.
14. Kulikov, G.M. Finite deformation plate theory and large rigid-body motions / G.M. Kulikov, S.V. Plotnikova // International Journal of Non-Linear Mechanics. – 2004. – Vol. 39. – P. 1093–1109.

---

### Гибридные четырехугольные трехмерные элементы пластины. Оценка и новые подходы

Г.М. Куликов, С.В. Плотникова

*Кафедра «Прикладная математика и механика», ГОУ ВПО «ТГТУ»*

**Ключевые слова и фразы:** гибридные конечно-элементные модели; метод введенных локальных деформаций; четырехузловой трехмерный элемент пластины.

**Аннотация:** На основе трехмерной теории пластин первого порядка, предложенной ранее авторами, построены гибридные четырехузловые ANS элементы пластины с введенными распределениями напряжений и деформаций. Все гибридные трехмерные элементы пластины основаны на общей методологии, что дает возможность оценить их достоинства и недостатки. Например, гибридный четырехугольный ANS элемент с введенными распределениями напряжений и деформаций позволяет использовать аналитическое интегрирование, которое приводит к очень простой структуре его матрицы жесткости. В то же время гибридный четырехугольный ANS элемент с введенным распределением напряжений демонстрирует превосходную производительность во всех рассмотренных тестовых задачах, но требует численного обращения матрицы большой размерности.

---

### **Hybride viereckige dreidimensionale Plattenelemente. Einschätzung und neue Behandlungen**

**Zusammenfassung:** Auf Grund der dreidimensionalen von den Autoren früher vorgeschlagenen Plattentheorie der ersten Ordnung sind die hybriden vierknotigen ANS Plattenelemente mit den eingeführten Spannungsverteilungen und mit der Deformierung gebaut. Alle hybriden dreidimensionalen Plattenelemente sind auf die gesamte Methodologie gegründet, was die Möglichkeit ihre Vorteile und Nachteile einzuschätzen erlaubt. Zum Beispiel, das hybride viereckige ANS Element mit den eingeführten Verteilungen der Spannungen und der Deformationen erlaubt, die analytische Integration zu verwenden, die zur sehr einfachen Struktur seiner Matrix der Härte bringt. Gleichzeitig demonstriert das hybride viereckige ANS Element mit der eingeführten Verteilung der Anstrengungen die ausgezeichnete Produktivität in allen betrachteten Prüfungsaufgaben, aber fordert die numerische Behandlung der Matrix der großen Dimension.

---

### **Éléments quadrilatéraux hybrides tridimensionnels des plaques. Évaluations et nouvelles approches**

**Résumé:** A la base de la théorie des plaques du premier ordre proposée par les auteurs auparavant sont construits des éléments hybrides à quatre noeuds ANS avec l'introduction des répartitions des tensions et des déformations. Tous les éléments hybrides tridimensionnels de la plaque sont fondés sur une méthode commune ce qui permet d'évaluer leurs qualités et leurs défauts. Par exemple, l'élément quadrilatéral ANS avec l'introduction des répartitions des tensions et des déformations permet d'utiliser l'intégration analytique qui aboutit à une très simple structure de sa matrice de rigidité. En même temps, l'élément hybride quadrilatéral ANS avec l'introduction des répartitions des tensions montre une excellente productivité dans tous les problèmes de test examinés, mais demande une conversion numérique de la matrice de grande dimension.

---